Iranian Journal of Astronomy and Astrophysics
Vol. 5, No. 1, Spring 2018

DOI:10.22128/ijaa.2018.141

Iranian Journal of Astronomy and Astrophysics

Slip distribution of the 2010 August 27 Mw 5.8 Kuh-Zar earthquake from finite-fault modeling

Sonia Bazargan[1] · Nazila Asaadi[2] · Zaher Hossein Shomali[3] · Mehdi Rezapour[4]

[1] Institute of Geophysics, University of Tehran, Tehran, Iran;
email: bazargan.s@alumni.ut.ac.ir
[2] Department of Physics, Zanjan University, Zanjan, Iran;
email: nazilaasaadi@znu.ac.ir
[3] Institute of Geophysics, University of Tehran, Tehran, Iran;
email: shomali@ut.ac.ir
[4] Institute of Geophysics, University of Tehran, Tehran, Iran;
email: rezapour@ut.ac.ir

Abstract. The slip distribution of a moderate earthquake of Iran, the 27th of August, 2010 Mw 5 : 8 Kuh-Zar earthquake, was estimated from regional broadband seismic data using constrained non-negative least squares linear slip inversion method. A great many inversions were carried to determine the optimal parameters used in the process such as rupture velocity and rise time. A rupture velocity of 2.55 km/s and rise time of 1.8 s were utilized for the event. Results show a rupture with peak slip of 15.0 cm and total seismic moment release of 2×10^{25} dyne-cm. The effect of the stations with different epicentral distances was also analyzed using a sensitivity test. Due to the non-uniqueness of the inversion problem, a set of solutions is presented for the Kuh-Zar earthquake. To the best of our knowledge, this is the first time to consider constrained non-negative least square linear finite-fault inversion procedure to the Kuh-Zar earthquake.

Keywords: the 2010 Juh-Zar earthquake, seismic data, slip inversion

1 Introduction

This study is focused on acquiring spatial slip distribution of the 27th of August, 2010 Mw 5 : 8 Kuh-Zar earthquake which occurred in Kuh-Zar, a village in Damghan county, Semnan Province (Fig. 1). Based on the seismic zoning of Iran by Mirzaei et al. (1998) [1], there are five major seismotectonic provinces in the country, that is Zagros in the southwest, Alborz-Azerbaijan in the north and northwest, Central East Iran, Kopeh Dagh in the northeast and Makran in the southeast of Iran. The Kuh-Zar earthquake is almost situated on the border of Alborz-Azerbaijan and central East Iran seismotectonic provinces which is in the proximity of the southern border of Alborz region. The epicenter of this event is located north of the Torud fault which is the causative fault for the 1953 Torud earthquake [2], one of the remarkable events of this area. Although the earthquake magnitude is moderate, it affected 12 villages i.e. Kuh-Zar, Salmabad, Tuchahi, Kelu, Shemi, Bidestan, Hoseynian, Moalleman, Satveh, Reshm, Mehdiabad, and Torud, which all are situated in Semnan Province. The study aimed to obtain finite-fault modeling of the broadband three-component displacement waveforms of the Kuh-Zar earthquake through a least squares inversion method for the spatial slip distribution.

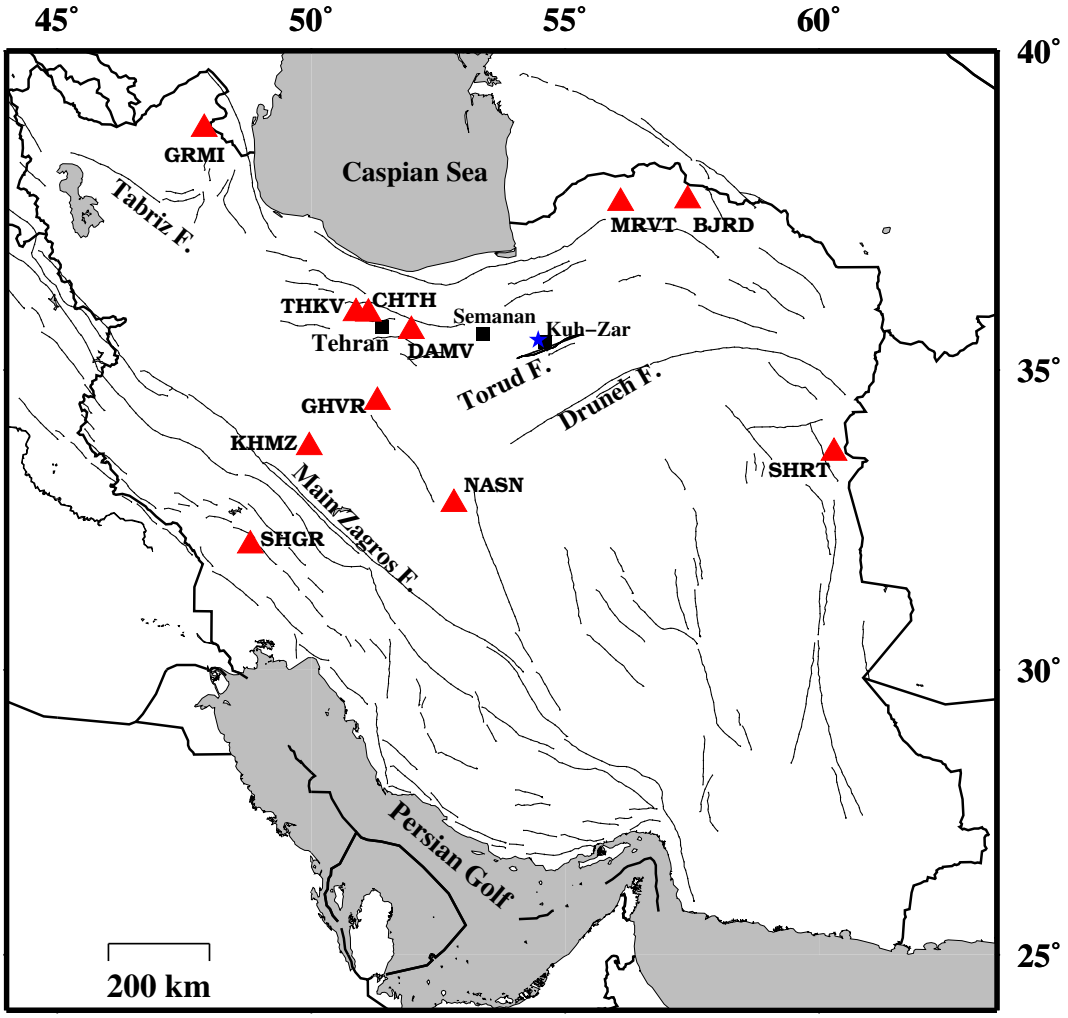

Figure 1: Distribution of stations for the Kuh-Zar earthquake. Location of the epicenter is given by the blue star. Solid lines demonstrate fault traces of Iran. Three major faults of Iran such as Daruneh and Main Zagros faults are illustrated in the figure. Also, the Torud fault is shown in the south of the epicenter. Black squares symbolize Tehran and Semnan provinces, and Kuh-Zar village. The event is almost situated on the border of Alborz-Azerbaijan and Central East Iran seismotectonic provinces which in the vicinity of Semnan province near Tehran.

Table 1: Recording stations and their epicentral distances.

Station names	Epicentral Distance (km)
damv	229.632
mrvt	280.236
chth	308.302
ghvr	312.472
thkv	330.817
nasn	336.096
khmz	458.895
shrt	569.186
shgr	646.726
grmi	692.948

2 Data

The data used in this study is obtained from national broadband seismic network operated by International Institute of Earthquake Engineering and Seismology of Iran (IIEES, www.iiees.ac.ir). These data consist of 26 waveforms for the 27th of August, 2010 Mw 5 : 8 Kuh-Zar earthquake. Fig. 1 shows the location of the stations. The stations and their epicentral distances are listed in Table 1. The aftershocks of the correspondng earthquakes were taken from the catalog of Iranian Seismological Center (IRSC, irsc.ut.ac.ir). The observed waveforms were filtered and decimated from original 50 to 10 sampels per second. The instrument responses were removed, and the data were then converted to displacement. A band-pass filter of $0.025 - 0.07$ Hz was applied to the displacement waveforms.

3 Modal Parameterization

Green's functions were computed using the frequency-wavenumber integration code (FKRPROG) developed by Saikia (1994) [3]. The inversion algorithm applied to the observed data is based on a stabilized constrained non-negative least-square method introduced by Hartzell and Heaton (1983) [4].

The optimal values of the input parameters are obtained as a result of running plenty of inverions. Fault and subfault sizes are the first parameters constructing our parameterization. In this spatial distribution, the model parameters compose a single fault segment with smoothing stabilization. The key point is that large subfaults may produce artifacts. Also, slip models with the lack of spatial resolution of the fault details can be obtained by a few large subfaults [4]. Furthermore, using very small subfaults may produce completely erroneous results with slip patches which are probably artifacts. In this regard, we tested different subfault sizes in the range from 0.5 km to 3.0 km to find the best choice. After lots of inversion trials, we found the equal-sized 2 km $\times$ 2 km subfault with a surface of 48 km by 48 km accommodate all of the slip distribution inside the given fault plane. Also, this size has enough resolution of fault details with a maximum percentage of fitting between observed and synthetic data.

Non-uniqueness of the inversion problem led us to prepare a set of solutions. Therefore, we used different hypocentral parameters and focal mechanisms. Different hypocenters reported by various seismological agencies, i.e., ISC, GCMT, USGS, and EMSC (Table 2)

Table 2: The hypocentral parameters recorded by different agencies for kuh-Zar earthquake.

*Agencies**	Lat.(°)	Lon.(°)	Depth (km)	Time
ISC	35.48	54.50	11.0	$19^h23^m48^s.87$
GCMT	35.53	54.49	14.9	$19^h23^m52^s.40$
USGS	35.49	54.47	7.0	$19^h23^m49^s.00$
EMGS	35.48	54.55	10.0	$19^h23^m48^s.30$

∗ ISC (www.isc.ac.uk), International Seismological Center;
GCMT (www.globalcmt.org), Global Centroid Moment Tensor;
USGS (www.earthquake.usgs.gov), United States Geological Survay;
EMSC (www.emsccsem.org), European-Mediterranean Seismological center

Table 3: The focal mechanisms reported by GCMT and NEIC.

2010 Kuh-Zar	Nodal plane 1 Srtike (°), Dip(°), Dike(°)	Nodal Plane 2 Strike(°), Dip(°), Dike(°)
GCMT	212, 78, -2	302, 88, -168
*NEIC**	20, 85, -10	111, 80, -175

∗ The National Earthquake Information Center

were tested. Since the nodal plane with a better fit to the data can be construed as the main fault plane [5], the focal mechanism (strike, dip, and rake) of the fault reported by GCMT and NEIC were tested to find the nodal plane with the best fit (Table 3). And, the resulting models helped us to determine the fault plane from the auxiliary plane. The measure to choose the optimal result in all runs has been total variance reduction –demonstrating the fit between observed and synthetic data– and the final variance of the data misfit. As a result, the inversion found better fits with strike equals to 212° nodal plane of GCMT (Table 3); thus, this plane is the fault plane, and we used it for the rest of the investigation.

Another significant parameter is rupture velocity. The rupture velocity was assumed to be a constant fraction of the shear wave velocity at source area, and we tested different values of this parameter in a range of 0.7 to 0.9 of the shear wave velocity.

Stabilization constrains, that are moment minimization and smooth weight, are another parameters in the inversion that reduce instability or extreme complexity. To choose the optimal results, we tested different amounts of these constraints to find the best values that yield a smooth slip modal with the minimum seismic moment [4].

4 Results

The velocity model based on the study of Ashtari et al. (2005)[7] was used for this event. We determined several spatial slip distributions for the Kuh-Zar earthquake by using different hypocentral parameters (Table 2). According to these models (Fig. 2), distribution of slip is critically sensitive to the depth of hypocenter. GCMT and USGS hypocnters (Table 2) were found to provide the best fit to the observed data with maximum total variance reduction of about 44% for spatial distribution, but the variance of the data misfit obtained by GCMT is the least. Moreover, USGS hypocenter gave a slip pattern with surface fault rupture

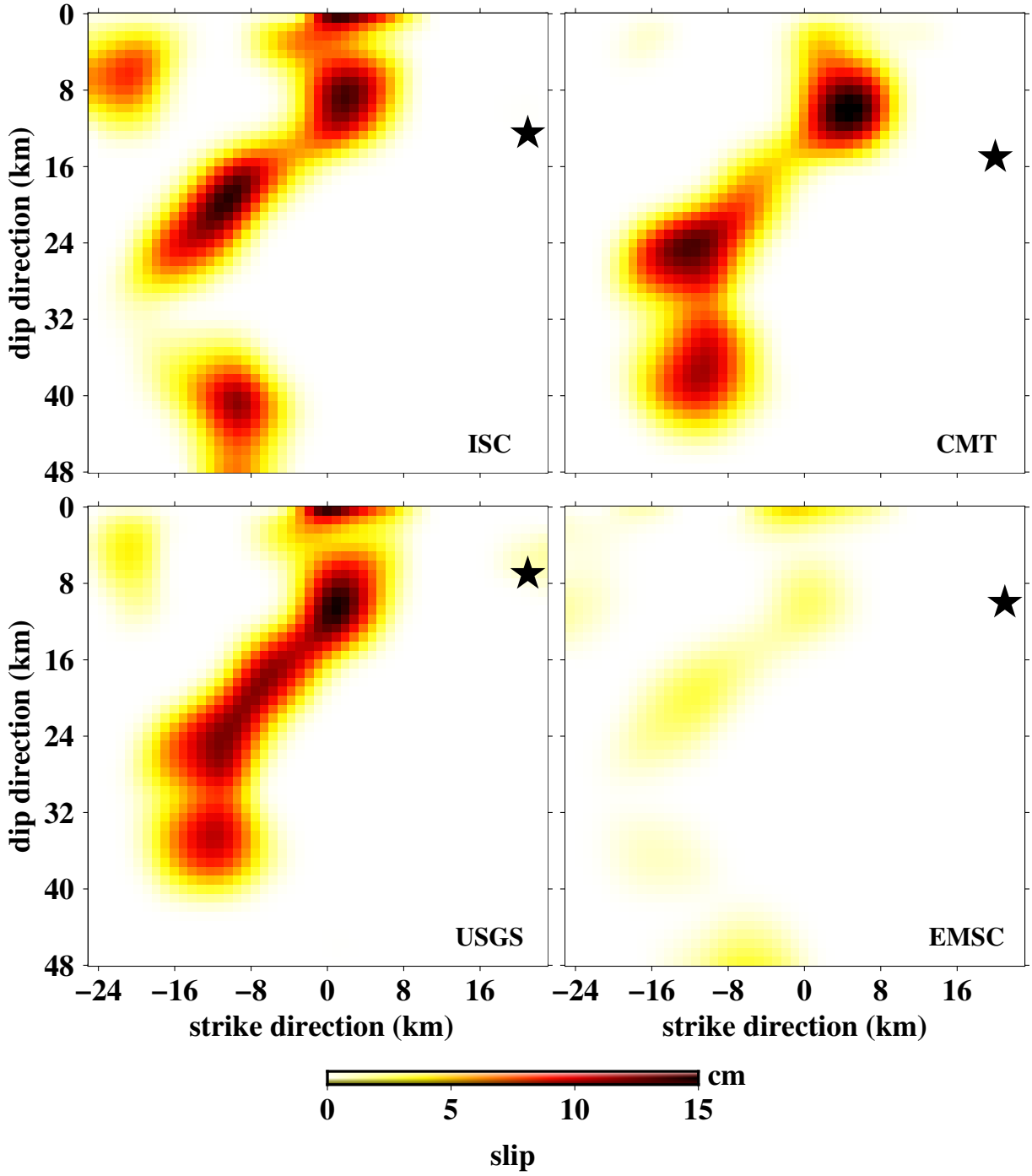

Figure 2: A set of solutions for the spatial slip distribution of the Kuh-Zar earthquake using different seismological agencies–ISC, GCMT, USGS, and EMSC (see Table 2). Black stars show the hypocenter of the ISC (top, left), GCMT (top, right), USGS (bottom, left), and EMSC (bottom, right) in each box. Our preferred model for this event is obtained by the GCMT hypocenter with maximum total variance reduction of 44% and minimum variance of the data misfit. The peak slip value in all models is scaled to 15.0 cm –the peak slip value of the preferred slip model.

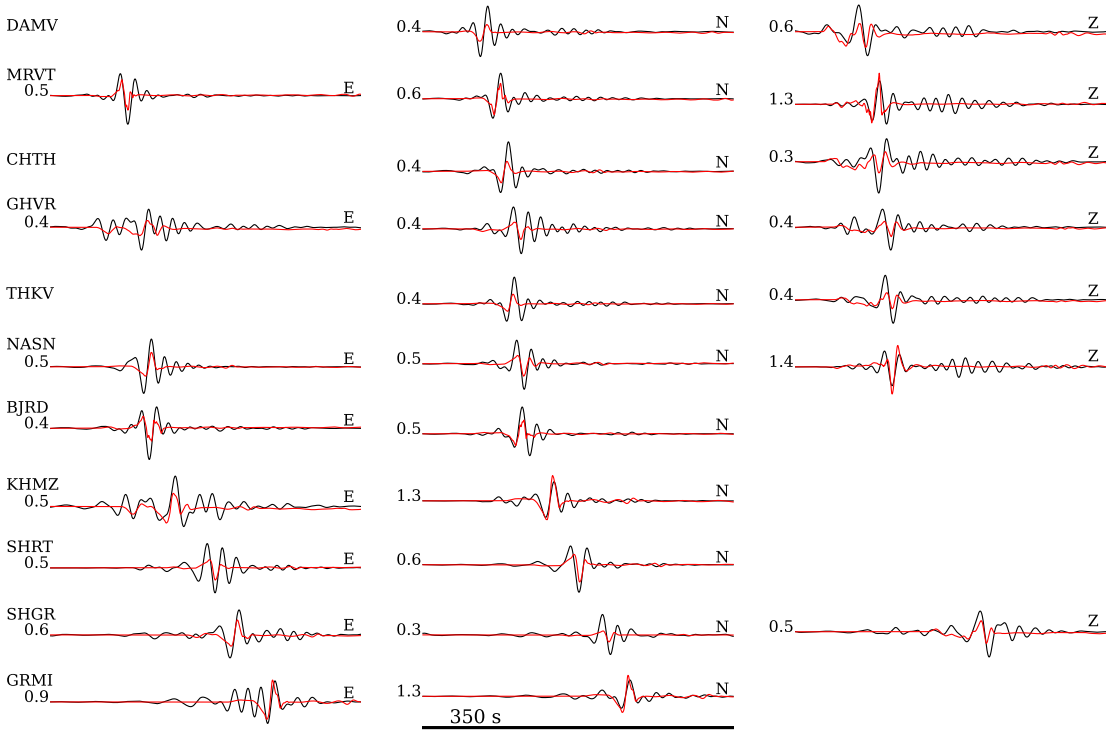

Figure 3: Observed data (black) and synthetics (red) for the spatial slip distribution of the Kuh-Zar earthquake with respect to our preferred model with total variance reduction of 44%, rupture velocity of 2.55 km/s and rise time of 1.8 s obtained from GCMT hypocenter and focal mechanism. E component of DAMV, CHTH, and THKV, and Z component of BJRD, KHMZ, SHRT, and GRMI were omitted because we could not satisfactorily fit the signals due to the presence of noise. Numbers on the left of each signal pair show the synthetic to observed amplitude ratio. Signals are displayed in order of increasing the distance from the epicenter.

which has not been corroborated by Shahvar and Zare (2013)[6]. Furthermore, all of the hypocenter except GCMT provided models which are not covering all of the slip distribution inside the given fault plane because of their lower depths (EMSC hypocenter has the least variance reduction and its peak slip is 6 cm). Therefore, slip pattern acquired by GCMT hypocenter is chosen as the preferred spatial slip model of Kuh-Zar earthquake (Fig. 2). Based on the preferred model, the peak slip is almost 15 cm, and the total seismic moment release is about 2.0×10^{25} dyne-cm.

The rupture velocity of 2.55 km/s provided the best fit to the data. It indicates that the rupture front propagated with a rupture velocity as 70 percent as the shear wave velocity in the source area. Based on lots of inversion trials, rupture velocities higher than 2.55 km/s failed to explain the rupturing well. In accord with different inversion runs, optimum rise time was also chosen to be 1.8 sec. The spatial distribution of the preferred slip model illustrates an asperity centered west of hypocenter (Fig. 2).

Fig. 3 demonstrates the observed data and synthetics. East-west component of DAMV, CHTH and THKV stations, and Z component of BJRD, KHMZ, SHRT and GRMI stations were omitted because we could not acceptably fit the waveforms due to the presence of noise.

5 Sensitivity of the results

The sensitivity of the final slip model of Kuh-Zar earthquake to the data set was investigated by dividing stations into different groups and inverting the data accordingly. By so doing, we analyzed the effect of the distribution geometry of stations on the final slip model. For this mean, two scenarios were defined as follows. In the beginning, inversion was conducted for stations separated into two groups representing near and far ones based on their epicentral distances (Table 1). Secondly, the inversion was once run only by considering componet E, N, and Z of all stations exclusively. When we run inversion for the spatial distribution of Kuh-Zar earthquake by considering near and far stations (the first scenario), we found that running inversion with only near stations gives the whole slip pattern of the final model; while, the far ones just give the south patch of the final model with small amount of slip. This indicates that near stations play a crucial role in creating the slip pattern.

In second scenario, mean amplitude of N components is larger than E components, but E components have better fits to the data. Also, Z componenets have the lowest mean amplitude and the worst fitting.

6 Discussion

The Kuh-Zar earthquake is one of the moderate earthquakes of Iran whose slip distribution is explored by linear finite-fault slip inversion method. The research, which is considered at nearly low frequencies, resulted in the main features of slip distribution of the event.

We presented a set of solutions for the earthquake, among which GCMT hypocenter and focal mechanism give the best spatial distribution with a maximum total variance reduction of 44%. The peak slip value of this event is about 15.0 cm. Also, the main nodal plane is one which provided the maximum total variance reduction in the slip inversion. For the Kuh-Zar earthquake, the fault plane with strike, dip, rake: 212°, 78°, −2° satisfied this condition.

According to the lots of inversion trials, rupture velocity is a major contributor to slip inversion. The observed data were re-inverted for different rupture velocities, among which 2.55 km/s gives the best result with maximum total variance reduction and minimum vari-

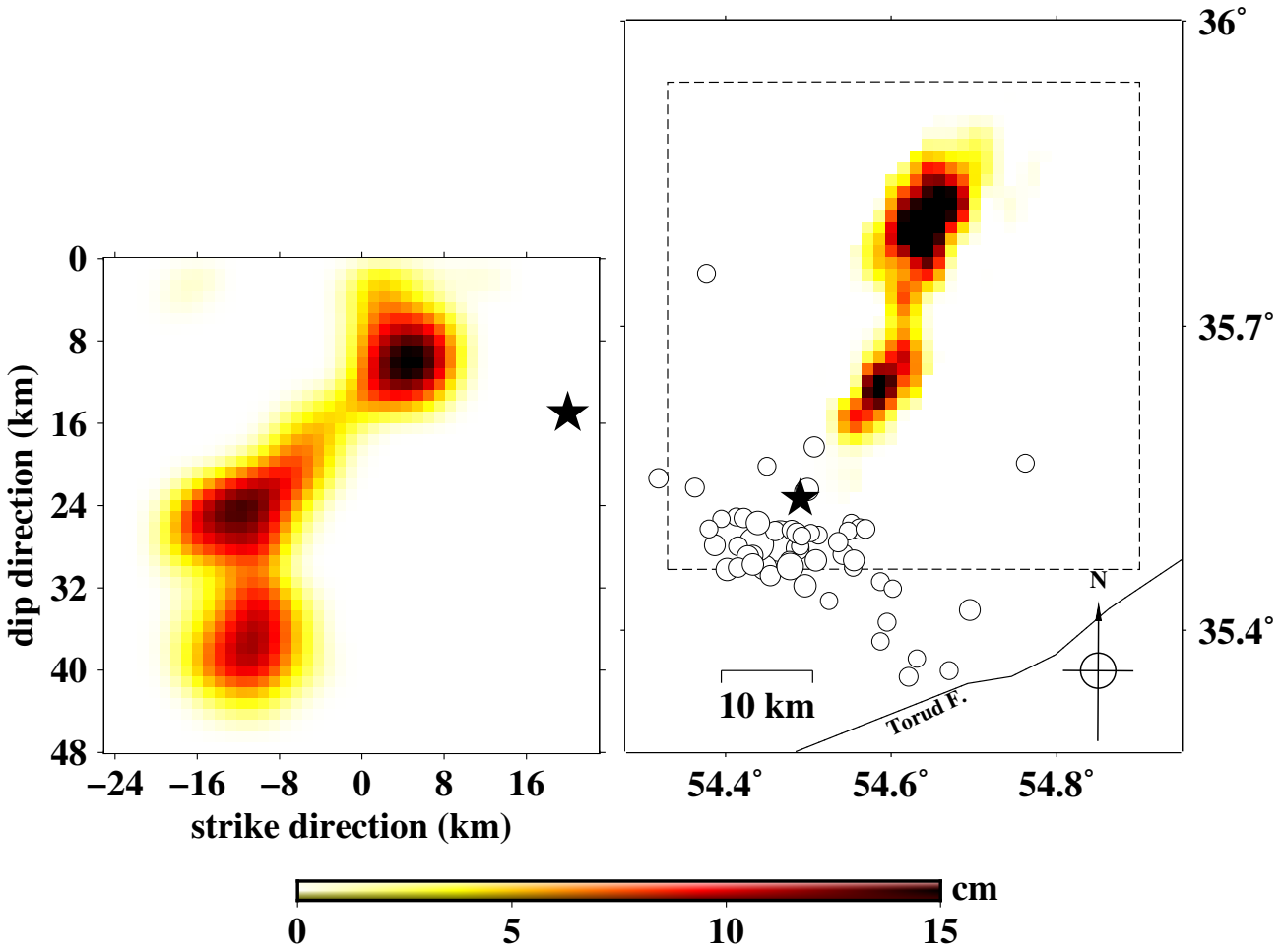

Figure 4: Slip distribution of the preferred finite-fault models for the Kuh-Zar earthquake in the latitude-longitude coordinate (right) and along strike-dip directions (left). The dashed square (right) presents the fault plane (with the strike of 212° 212) on the earth. Black stars show GCMT hypocenters in both figures. The white circles refer to the aftershocks which occurred during a month after the main shock and were taken from the catalog of Iranian Seismological Center (IRSC). The aftershocks distribute outside of the asperity zone. The peak slip value of the event is 15.0 cm. Also, the Torude fault has been shown in a black line (right) situated south of the slip distribution.

ance of the data misfit. Moreover, as rupture velocity increases, the slip is distributed further out of the htpocenter for the Kuh-Zar earthquake which is in agreement with Hartzell et al. (2007) [8] sensitivity tests results for the 2004 Parkfield, California earthquake. Rise time is another effective parameter in our study, and the slip distribution is found to be sensitive to different values of it. As rise time increases, the waveforms become more smooth. The rise time of 1.8 s gives the best synthetics in terms of smoothness.

According to the sensitivity test, the distribution is sensitive to the number of stations and their azimuthal gap. The same result was obtained by Hartzell et al. (2007) [8] for the 2004 Parkfield, California earthquake. Furthermore, epicentral distances of the stations are a significant contributor to the slip distribution, that is far stations are not so influential in the final peak slip.

Fig. 4 (right) shows analogies between the projected final spatial distribution on the Earth surface with the aftershock dsitribution (one month after the main shock). The dashed square depicts the whole region of the fault plane. Aftershocks are a phase of relaxing stress concentrations followed by a mainshock [9, 10] and occurred southwest of the slip distribution for the Kuh-Zar earthquake. It is shown that the aftershocks distribute mostly outside of the asperity zone. The same results have been acquired in some studies including Doster and Kanamori (1986) [11], Hartzell and Heaton (1986) [12], Mendoza and Hartzell (1988) [13], and Reasenberg and Ellsworth (1982) [14].

References

[1] Mirzaei, N., Mengtan, G., & Yuntaim, C. 1998, J. Earthq. Predic. Res., 7, 465

[2] Berberian, M., & Navai, I., 1977 A preliminary feild report and a seismotectonic, 40, 51

[3] Saikia, C. K. 1994, Geophys. J. Int., 118, 142

[4] Hartzell, S. H., & Heaton, T. H. 1983, Seismol. Soc. Am., 73, 1553

[5] Abercrombie, R. E., Bannister, S., Pancha, A., Webb. T. H., & Mori, J. J. 2001, Geophys. J. Int., 146, 134

[6] Shahvar, M. P., & Zar'e M., 2013, Nat. hazards, 66, 689

[7] Ashtari, M., Hatzfeld, D., & Kamalian, N. 2005, Tectonophysics, 395, 193

[8] Hartzell, S. H., Liu, P., Mendoza, C., Ji, C., & Larson, K. M. 2007, Seismol. Soc. Am., 97, 1911

[9] Scholz, C. H. 1990, Cambridge Univ. press, 146, 134

[10] Lay, T., & Wallace, T. C. 1995, Modern global seismology, Academic Press, San Diego

[11] Doser, D. I., & Kanamori, H. 1986, Geophys. Res., 91, 675

[12] Hartzell, S. H., & Heaton, T. H. 1986, Seismol. Soc. Am., 76, 649

[13] Mendoza C., & Hartzell S. H. 1988, Seismol. Soc. Am., 78, 1438

[14] Reasenberg, P., & Ellsworth, W. L. 1982, J. Geophys. Res., 87, 10637